

Sliding and Abrasive Wear Resistance of Thermal-Sprayed WC-Co Coatings

Yunfei Qiao, YouRong Liu, and Traugott E. Fischer

(Submitted 12 January 2000)

We studied the resistance of the coatings to abrasive and unlubricated sliding wear of 40 WC/Co coatings applied by high velocity oxygen fuel (HVOF), high-energy plasma spray (HEPS), and high velocity plasma spray (HVPS), using commercial and nanostructured experimental powders. The hardness of the coatings varies from 3 to 13 GPa, which is much lower than that of sintered samples (10 to 23 GPa) because of the porosity of the coatings. Phase analysis by x-ray diffraction revealed various amounts of decarburization in the coatings, some of which contain WC, W_2C , W, and η phase. The abrasive and sliding wear resistance is limited by the hardness of the samples. For a given hardness, the wear resistance is lowered by decarburization, which produces a hard but brittle phase. Nanocarb powders have the shape of thin-walled hollow spheres that heat up rapidly in the gun and are more prone to decarburization than commercial materials. The work shows that, in order to obtain the performance of nanostructured coatings, the powder and spray techniques must be modified.

Keywords nanostructured coatings, process variables, wear morphology, wear resistance

1. Introduction

The work presented is part of a research program aimed at exploring the possible advantages of nanometer scale microstructures in WC/Co coatings. Previous work with bulk cermets sintered from nanostructured powders that were prepared by spray drying^[1] has shown that decreasing the WC crystal size results in higher hardness^[2] and increased resistance to sliding^[3] and abrasive wear.^[4] Naturally, these results suggested that the advantages of finer crystal structure could also be obtained in coatings that are applied to metallic substrates by the thermal spray method.

The powders used in this technology consist of a mixture of WC grains and cobalt, which are agglomerated into particles large enough to flow in the spray equipment.^[5-10] These particles are partially molten and projected on the substrate by a plasma or high-velocity flame gun.^[5,7,11-19] The adhesion and properties of the coatings depend on the amount of partial melting of the particles and on the energy (velocity) with which they impinge on the substrate.^[7,8,20] A very high temperature to which the particles are subjected and, to a certain extent, the chemical reaction with the flame (oxidation) cause not only melting but chemical and structural changes in the material. These changes are decarburization of WC to W_2C ^[6,7,14] or even tungsten and formation of an η phase (W_xCo_yC); dissolution of W and C in the Co; formation of an amorphous Co binder phase because of the rapid cooling on the substrate; and loss of Co and C due to evaporation or

oxidation.^[5,11,12-27] These chemical transformations produce brittle phases that reduce the toughness on a macroscopic or microscopic scale and reduce wear resistance.^[7-9,12,21-27] Decarburization can be reduced with a fuel producing sufficient carbon activity in the flame.^[8] A low temperature produces insufficient melting of the particles, which results in porosity and poor adhesion between splats. The consequence is insufficient hardness of the coating and low wear resistance.^[1]

The above discussion shows that it is inevitable that WC/Co coatings have lower hardness and wear resistance than sintered bulk cermets. However, the performance of these coatings is still much better than that of their steel substrates. The lower hardness of the coatings has the major advantage that they adhere well to the substrate: failure of the coating by debonding from the substrate is usually not a problem.

To date, the defects introduced by the spray processes dominate the wear mechanisms and the expected increases in hardness, and wear resistance of the nanostructured materials has not been achieved. To the contrary, the use of nanostructured powders has produced inferior coatings.^[22] This, however, is not inherent in the WC grain size but is a consequence of the morphology of the agglomerated particles, which have had the shape of hollow thin-walled shells^[27] that heat up to excessive temperatures in the gun.

The above conclusions were drawn from studies^[5-31] that each examined a small number of coatings and usually included only one parameter that varied at a time. Most wear rates are given in relative values and do not allow for comparison between the results of different authors. In the present paper, we have examined a large number of coatings that several laboratories have prepared by high velocity oxygen fuel (HVOF), high-energy plasma spray (HEPS), and high-velocity plasma spray (HVPS) methods, using either commercial (Diamalloy 2004 (Sulzer Metco, Westbury, NY)) or experimental nanostructured powders as feed. We have measured the resistance of these coatings to wear in unlubricated sliding and in abrasion tests. The results are related to the hardness of these samples and discussed in

Yunfei Qiao, YouRong Liu, and Traugott E. Fischer, Department of Chemical, Biochemical and Materials Engineering, Stevens Institute of Technology, Hoboken, NJ 07030. Contact e-mail: tfischer@stevens-tech.edu.



Table 1 Chemistry, hardness, microstructure, sliding wear, and abrasive wear of WC/Co coatings

Sample	Powder	Powder metal content (Co,Ni,Cr) (%)	Spray tech.	Spray gun	Grain size (μm) (coating)	WC (%)	W ₂ C (%)	W (%)	HV _{1kg} (kg/mm ²)	Sliding wear rate ×10 ⁻⁶ mm ³ /N m	Abrasive wear rate ×10 ⁻² mm ³ /N m
SN1 ⁴	Nano & Conv.	9.9	HVOF	Std DJ	0.3–2.0	98.5	1.5	0	350	0.60	2.10
SN2 ⁴	Nano & Conv. + Metglas	10	HVOF	Std DJ	0.3–2.0	98.3	1.7	0	320	0.55	0.80
SC3	Diamalloy ² 2004	12	HVOF	Std DJ	0.6–3.0	99.0	1.0	0	320	0.50	1.60
SC1 ⁴	Nano & Conv.	9.9	HVOF	Std DJ	0.3–2.0	99.5	0.5	0	760	0.30	0.60
SC2 ⁴	Nano & Conv. + Metglas	10	HVOF	Std DJ	0.3–2.0	97.0	2.0	1.0	720	0.27	0.70
SF3	Nanocarb ¹	8	HVOF	Std DJ	0.2–0.3	30.0	12.6	57.4	780	0.40	2.30
SF4	Nanocarb + Metglas	10	HVOF	Std DJ	0.2–0.3	51.0	23.2	25.8	350	0.38	2.00
SC5 ⁴	Nano & Conv.	9.9	HVOF	Std DJ	0.3–2.0	97.7	1.3	0	820	0.15	0.40
SC6 ⁴	Nano & Conv. + Metglas	12.75	HVOF	Std DJ	0.3–2.0	98.7	1.3	0	840	0.30	0.95
SC7 ⁴	Nano & Conv.	7.1	HVOF	Std DJ	0.3–0.2	97.2	2.8	0	470	0.30	1.30
R6	Nanocarb ¹	15	HVOF	Std DJ	0.2–0.3	91.5	5.5	3.0	590	0.30	1.70
R24	Nanocarb ¹	15	HVOF	Std DJ	0.2–0.3	92.0	4.4	3.6	490	0.40	2.90
N83	Nanocarb ¹	8	HVOF	DJ2700	0.2–0.5	42.0	41.0	17.0	970	0.20	0.75
OS1	Osram-Sylvania ³ SX432	18	HVOF	DJ2700	0.2–0.5	67.0	33.0	0	1220	0.23	1.11
OS2	Osram-Sylvania ³ SX432	18	HVOF	DJ2700	0.2–0.5	66.0	34.0	0	1180	0.30	1.12
DJ1	Nanocarb ¹ (reprocessed by Inframat)	15	HVOF	DJ2700	0.2–0.5	31.0	17.5	51.5	1140	0.60	1.00
DJ2	Nanocarb ¹ (reprocessed by Inframat ⁶)	15	HVOF	DJ2700	0.2–0.5	5.5	36.0	58.5	1030	0.50	1.20
JK117	Osram-Sylvania ³	17	HVOF	Jet Kote	0.2–2.0	73.0	20.0	7.0	1300	0.13	0.70
N515	Nanocarb ¹	15	HVOF	DJ2700	0.2–0.5	73.3	26.7	0	1050	0.2	0.9
OS422	Osram-Sylvania ³	9	HVOF	Jet Kote	0.2–2.0	65.5	33.7	0.8	1090	0.2	0.9
BB1*	Praxair ⁵ WC106	12	HVPS	Gator-Gard	3.0–6.0	31.0	24.0	0	910	0.36	1.10
BN1	Nanocarb	15	HVPS	Gator-Gard	0.2–0.5	97.0	2.0	1.0	890	0.40	1.30
BB2*	Praxair ⁵ WC106	12	HVPS	Gator-Gard	3.0–6.0	33.0	27.0	0	873	0.40	1.30
BN2	Nanocarb ¹	15	HVPS	Gator-Gard	0.2–0.5	97.5	2.5	0	889	0.30	1.20
G6-1	Nanocarb ¹	6	HEPS	PlazJet	0.2–1.0	20.0	37.5	42.5	675	0.51	3.30
G6-2	Nanocarb ¹	6	HEPS	PlazJet	0.2–1.0	21.0	38.4	40.6	824	0.40	3.80
G6-3	Nanocarb ¹	6	HEPS	PlazJet	0.2–1.0	57.6	29.4	13.0	770	0.77	1.90
G6-4	Nanocarb ¹	6	HEPS	PlazJet	0.2–1.0	19.0	21.0	60.0	825	0.57	2.90
G15-1	Nanocarb ¹	15	HEPS	PlazJet	0.2–1.0	51.0	49.0	0	762	0.70	2.50
G15-2	Nanocarb ¹	15	HEPS	PlazJet	0.2–1.0	63.0	37.0	0	822	0.86	1.40
G15-3	Nanocarb ¹	15	HEPS	PlazJet	0.2–1.0	40.5	59.5	0	805	1.00	1.42
G15-4	Nanocarb ¹	15	HEPS	PlazJet	0.2–1.0	57.0	43.0	0	955	0.40	1.55
G15-5	Nanocarb ¹	15	HEPS	PlazJet	0.2–1.0	51.0	49.0	0	916	0.86	1.20
L-1	Diamalloy ² 2004 (reprocessed by UCI)	12	HVOF	DJ2700	0.2–1.5	93.4	4.0	2.6	1260	0.15	0.48
L-2	Diamalloy ² 2004 (reprocessed by UCI)	12	HVOF	DJ2700	No grain	1.0	0.3	98.7	920	0.30	1.62
ADJ27N	Nanocarb ¹ (reprocessed by Inframat)	8	HVOF	DJ2700	0.2–0.5	15.0	38.0	47.0	1020	0.57	1.47
ADJ271	Osman-Sylvania ² SX432	18	HVOF	DJ2700	0.2–0.5	85.0	15.0	0	1200	0.36	1.41
ADJ272	Diamalloy ² 2004	12	HVOF	DJ2700	0.2–1.5	90.0	10.0	0	1080	0.17	0.67
AST-1	Osram-Sylvania ³ SX432	18	HVOF	Std DJ	0.2–0.5	95.0	5.0	0	760	0.24	1.00
AST-2	Diamalloy ² 2004	12	HVOF	Std DJ	0.2–1.5	96.0	4.0	0	430	0.36	1.20
AST-3	Nanocarb ¹ (reprocessed by Inframat ⁶)	8	HVOF	Std DJ	0.2–0.5	13.0	53.0	34.0	620	0.54	2.40
Substrate	Steel	240	4.60	2.70

¹Nanocarb, Union Miniere, New Brunswick, NJ. ²Diamalloy 2004, Sulzer Metco, Westbury, NY. ³Osram Sylvania, Towanda, PA. ⁴Nanopowder Enterprises, New Brunswick, NJ. ⁵Praxair, Indianapolis IN. ⁶Inframat, North Haven, NJ.

terms of the porosity and the degree of decarburization and the microstructure of the coatings. Our investigation largely confirms the earlier findings that the properties and performance of the coatings depend at least as much on the details of the spraying process as on the composition and grain structure of the powders used. Its contribution is to provide insight into the relative effects of all the processing parameters. In particular, we find that the preparation of nanostructured powders must be modified and the spray process must be adapted to the morphology of the

novel nanostructured powders before the expected benefit of very small WC grain sizes can be obtained.

2. Samples and Experimental Methods

Forty WC-Co coatings, deposited by different groups with different size powders and different thermal spray techniques, were evaluated. They are listed in Table 1 together with the pow-

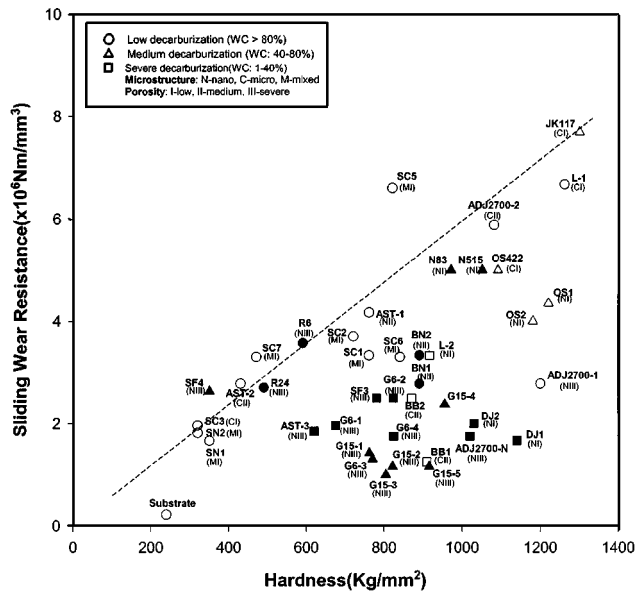


Fig. 1 Sliding wear resistance of the coatings as a function of hardness, decarburization, and porosity. Dark symbols denote samples sprayed with nanostructured powders in the form of hollow shells, and light symbols denote samples from commercial or experimental compact powders. The microstructures are those of the coatings, observed by SEM

ders and spray techniques, their microstructure, chemical composition, hardness, and tribological performance. The cobalt content indicated is nominal, as provided by the producer of the powder; it may differ from the actual amount in the powder and from that in the coating.

The surfaces of all samples were polished in three sequential steps: 30, 6, and 1 μm grade diamond lapping before all tests.

The microstructure on the surface and cross section of the coatings was observed under optical microscopy and scanning electron microscopy (SEM). X-ray diffraction analysis of the samples was conducted using $\text{Cu K}\alpha$ radiation at 40 kV and 20 mA. The phases were determined according to ASTM standards and their quantity was calculated from the integrated intensity of diffraction peaks.

The hardness on the surfaces and cross sections of the coatings were measured by Vickers indentations at 1000 g load. The values are between 2 and 20% lower than the hardness measured at 300 g, depending on the sample.

Sliding wear tests were conducted on a ball-on-disk tribometer at room temperature, in laboratory atmosphere, where WC-Co coated steel disk slides, without lubrication, against a commercial Si_3N_4 ball. The sliding speed was 30 mm/s and the load 9.8 N. The diameter of the traveling circle of the pin on the disk was 8 to 13 mm. The sliding distance was 10,000 to 12,000 m corresponding to 250,000 to 480,000 rotations of the disk. The volume of material removed was determined by measuring the cross section of the wear scar with a profilometer at several positions and averaging. The wear scars were studied by SEM.

The amount of material removed in sliding wear is proportional to the normal force on the ball in Newtons and the distance slid in meters; this allows us to define a wear rate in mm^3/Nm by dividing the volume of material lost by the sliding distance and the load. This is indicated in Table 1. The inverse of the wear

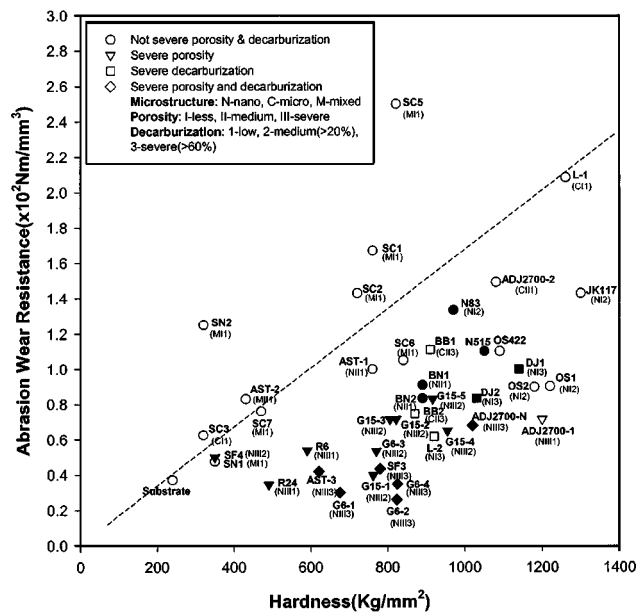


Fig. 2 Abrasive wear resistance of WC/Co coatings. Effect of hardness, porosity, decarburization, and microstructure. Dark symbols denote samples sprayed with nanostructured powders in the form of hollow shells, and light symbols denote samples from commercial or experimental compact powders. The microstructures are those of the coatings, determined by SEM

rate, in Nm/mm^3 , defines the wear resistance and is plotted in Fig. 1 and 2.

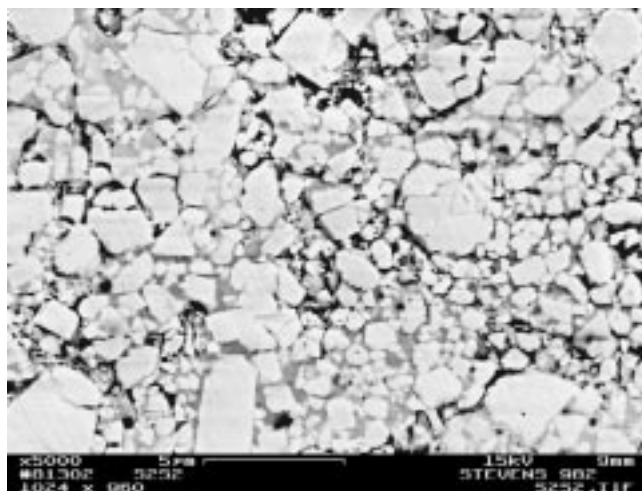
Abrasive wear was measured by sliding the samples against SiC abrasive bonded to a paper, under a load of 2 or 7 N over a distance of 38 m. The sample moved in a spiral on the abrasive sheet in order to encounter fresh abrasive during the entire test. The loss of material was determined by weighing the samples before and after the test. A density of $14 \text{ g}/\text{cm}^3$ was used to transform the mass into volume. Preliminary tests verified that the volume lost is proportional to the load and the sliding distance.

3. Results and Discussion

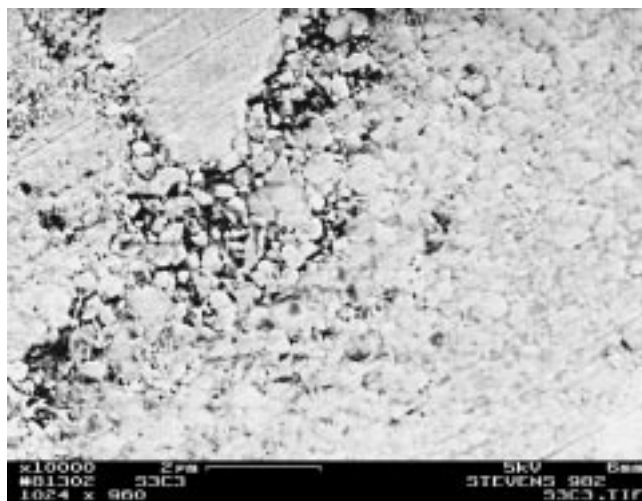
We first analyze the chemical composition, that is, the degree of decarburization of the samples; then we present the hardness and the resistance to sliding and abrasive wear of the coatings. Finally, we observe the microstructure and the wear scars of selected samples to obtain information on the wear mechanisms and the influence of the materials properties on them.

3.1 Phase Analysis

By measuring the integrated intensities of the WC-, W_2C -, W-, and η -phase peaks in x-ray diffraction, we find that the coatings undergo various extents of decarburization. The relative amounts of these phases are indicated in Table 1. The amount of Co cannot be determined accurately by x-ray diffraction and was not measured. In the coatings, the binder is amorphous^[8] and part of it is believed to be lost by evaporation.^[16] Li *et al.*^[8] and Takigawa *et al.*^[29] cite evidence that the flame enthalpy may be the



(a)



(b)

Fig. 3 Microstructure of (a) surface of sample SN2 and (b) cross section of sample R6. Submicron porosity due to lack of binder between the grains

primary driver for the initial decarburization reaction $WC \rightarrow W_2C$, while oxidation is responsible for further decarburization to tungsten. We found that the extent of decarburization also depends on the starting powders used. The decarburization degree of the coatings from Nanocarb powders is much greater than that of coatings produced with compact powders. This is due to the shape of the agglomerates more than to the size of the WC crystals: the hollow spheres of Nanocarb heat more rapidly in the flame than the compact agglomerates in the commercial powders.

3.2 Hardness

The data of Table 1 and Fig. 1 show that the hardness of the WC/Co coatings varies between 300 and 1200 kg/mm² (*i.e.*, between 3 and 12 GPa). This is much lower than the hardness of

bulk-sintered WC/Co, which ranges from 1100 to 2300 kg/mm² (11 to 23 GPa).^[2] Porosity is the most logical cause for low hardness, and this is confirmed by microscopic examination of the samples. The microstructures of two of the softer coatings SN2 (Hv = 320) and R6 (Hv = 590) in Fig. 3 show submicron porosity; lack of binder between the grains results in the low strength of these materials. However, we have not been able to establish a simple correlation between the porosity of the samples and their hardness. The presence of hard, brittle, decarburized W₂C phases and other aspects of the microstructure play a role in determining the hardness of the coatings.

3.3 Sliding Wear

The wear rate in unlubricated sliding against a silicon nitride ball at 9.8 N load is indicated in Table 1 and its inverse, the wear resistance (in Nm/mm³), is plotted against hardness in Fig. 1.

It is apparent that the wear resistance of the coatings is limited by their hardness; the highest wear resistance obtained increases linearly with hardness. For a given hardness, however, the wear resistance can be lower than the maximum value by as much as a factor of 4 due to the presence of brittle phases, especially W₂C. In Fig. 1, the symbols denote the extent of decarburization and porosity. It is apparent that the samples with severe decarburization or high porosity have lower wear resistance. It is worth noting that the WC/Co coatings present a sliding wear resistance superior to that of the steel substrate by a factor of 4 to 35.

Figure 4 shows the surface of sample OS2 with 66% retained WC (meaning that 34% of the original WC is decarburized) before and after wear. The unworn surface shows light areas that have a higher degree of decarburization. Guilemay *et al.*^[30] have shown that tungsten appears lighter than WC in SEM images due to the high atomic number of tungsten. Figure 4(b) shows, indeed, that the decarburized areas are worn more severely than the less decarburized ones. A high-resolution image of the wear scar (Fig 4c), viewed at near-glancing incidence, shows that the bottom of the worn areas is smooth, without traces of mechanical damage. Cracks roughly parallel to the surface are evident. The picture strongly suggests that material is removed by fracture along such cracks that propagate by fatigue with the numerous passages of the slider. By contrast, Fig. 4(d) shows the wear scar of coating ADJ272, which suffered relatively little decarburization and is more wear resistant (Fig. 1); in this case, wear occurs by attrition of individual WC grains.

3.4 Abrasive Wear

Figure 2 is a similar plot of the abrasion resistance (in Nm/mm³) of the same coatings. We note that abrasive wear is about 50,000 times faster than sliding wear.

The correlation with hardness is not as clear as in sliding wear. There is an upper limit for the abrasion resistance that increases with the hardness for most samples. However, the coatings with “multimodal” structures SN2, SC1, SC2, and SC5, which were sprayed from a mixture of 70% Diamalloy 2004 (Sulzer Metco, Westbury, NY) with micrometer WC grains and 30% nanostructured WC, have a resistance to abrasive wear that is higher than the maximum shown by the samples made from

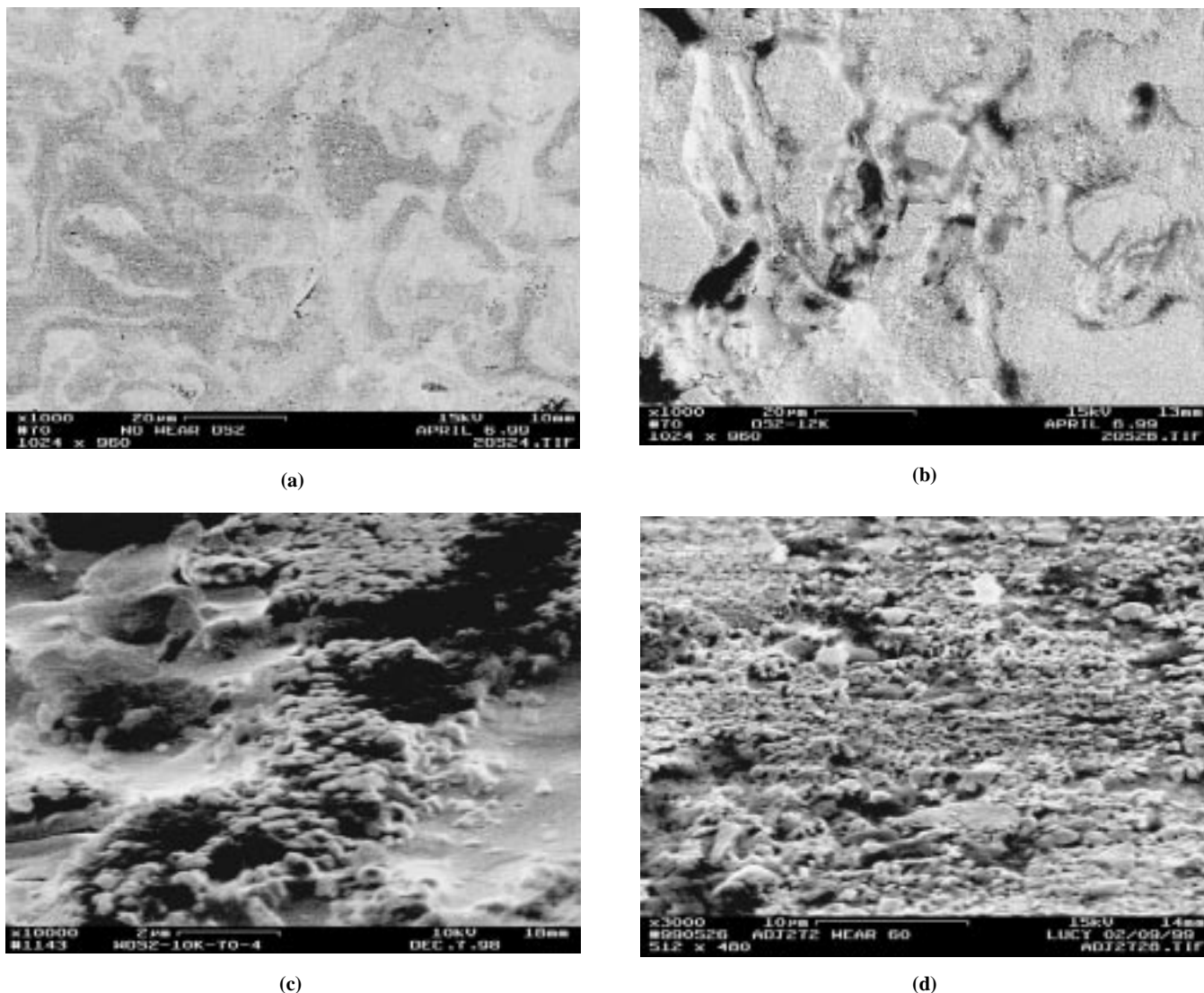


Fig. 4 SEM pictures of sample OS2 (a) before and (b) after wear in normal view. High-resolution 60° glancing angle (c) of OS2 and (d) of ADJ272. Light areas in (a) are decarburized; they are removed by wear in (b). Sample OS2 wears by fracture in decarburized regions, and sample ADJ272 wears by attrition of individual WC grains

homogeneous powders. The processing, properties, and performance of these bimodal materials are described in Ref 31. In general, we find again that severe decarburization is detrimental to the abrasive wear resistance.

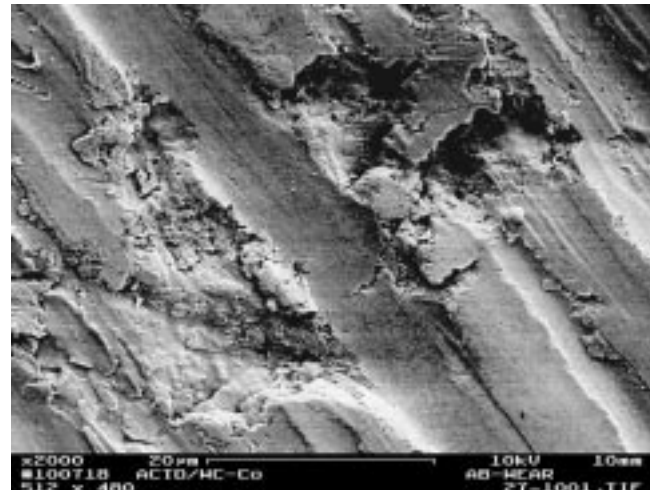
Figure 5 shows representative abraded surfaces, comparing surfaces with similar hardness but different abrasive wear. Figure 5(a) and (b) show two abraded materials with hardness around Hv 1300. Sample L1 (Fig. 5a) is one of the most abrasion-resistant materials. It has low porosity and very little decarburization. Sample ADJ271 has low abrasion resistance, 15% decarburization, and severe porosity (Table 1). Similarly, Figure 5(c) and (d) compare sample SC5 with G6-4. Their hardness is in the range of Hv 800. SC5 has a multimodal structure.^[31] G6-4 was sprayed with high-energy plasma; it suffered extensive decarburization (Table 1) because the powder was heated to high temperatures during deposition. The appearance of the

abraded surfaces in Fig. 5 provides clues for the differences in abrasion resistance. The two highly resistant surfaces (Fig. 5a and c) are smooth, with evidence of plastic deformation; the samples with low abrasion resistance (Fig. 5b and d) show extensive fracture. Obviously, brittle materials offer less resistance to plastic deformation than ductile ones of the same hardness. This is shown more emphatically in the scratches of Fig. 6. The scratches of samples L1 and SC5 (Fig. 6a and b) are clean and ductile. The scratch of sample G15 (which is similar to G6-4) is accompanied by large lateral cracks reminiscent of the ones seen with OS2 in Fig. 4(c).

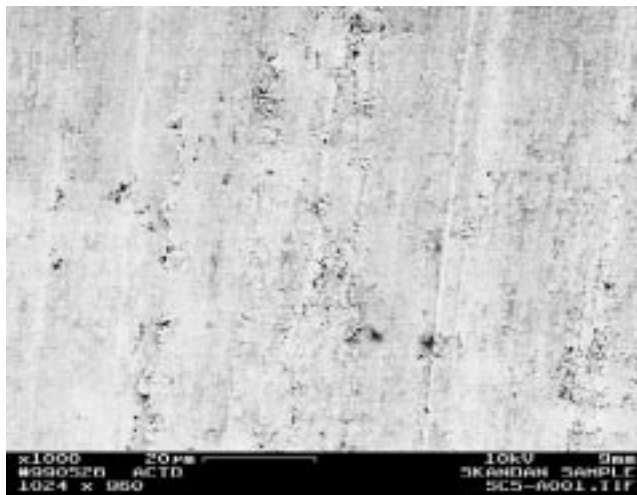
Krushov has already shown the importance of ductility in abrasion resistance in 1957^[32,33]: the abrasive wear resistance of metals is at least one order of magnitude higher than that of ceramics with similar hardness. In the former, the abrasive mostly forms plastic grooves, pushing the material around; in ceramics,



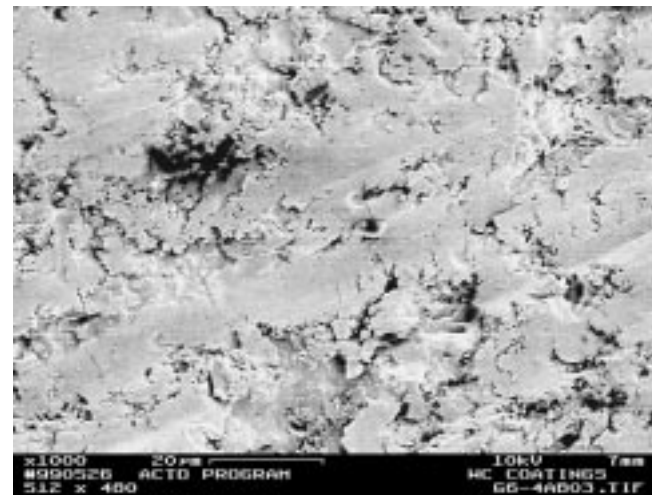
(a)



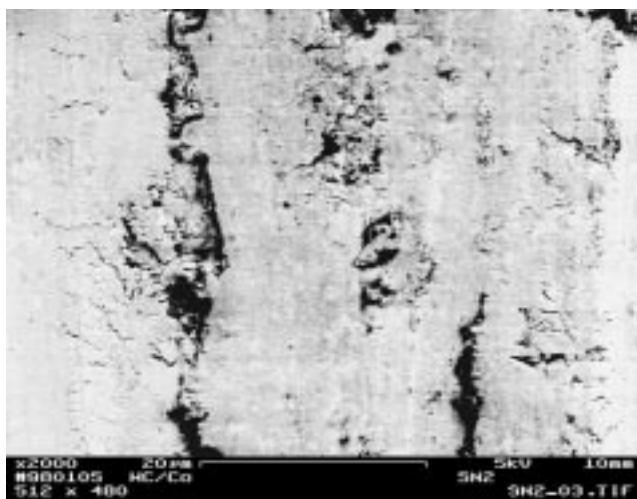
(b)



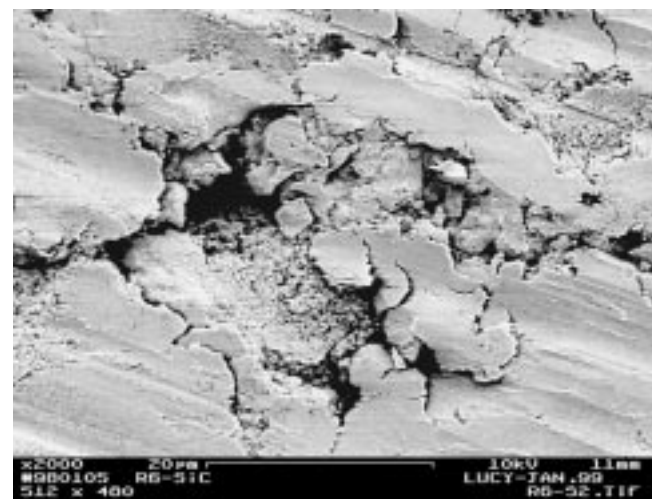
(c)



(d)



(e)



(f)

Fig. 5 Abraded surfaces of thermal-sprayed WC/Co coatings: (a) L-1 and (b) ADJ271 with hardness 1200 Hv; (c) SC5 and (d) G6-4 with hardness 820 Hv; and (e) SN2 and (f) R6 with low hardness. At every hardness, lower abrasion resistance is characterized by brittle fracture

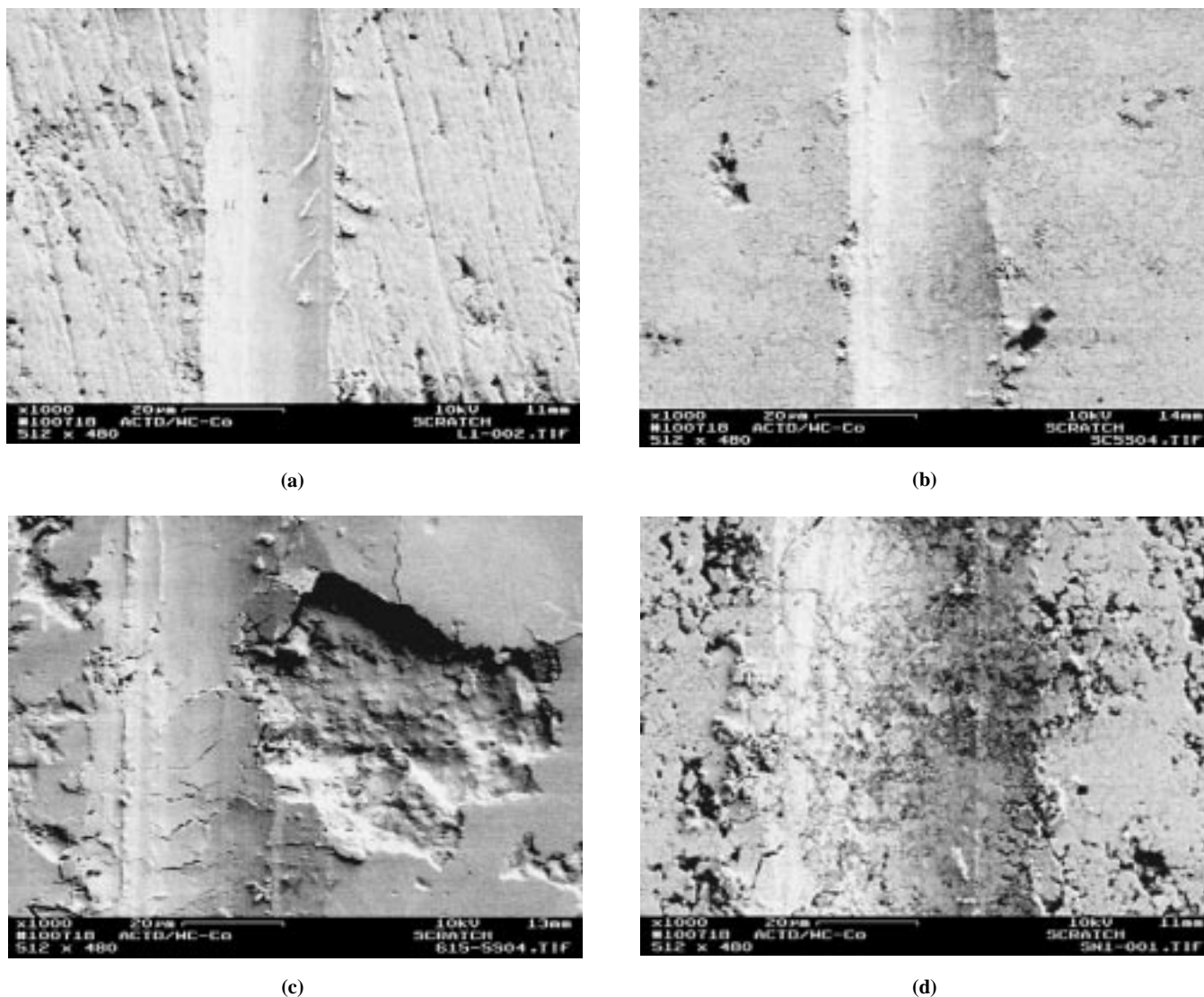


Fig. 6 SEM picture of the scratches on spray-coated WC/Co surfaces with a Vickers diamond at load 500g: (a) coating L-1, (b) coating SC5, (c) coating G15-5, and (d) coating SN2. The width of the scratches is a measure of the hardness. Note the ductility of L-1 and SC5, the fracture of brittle G15-5, and the crumbling of porous SN2

the groves are created by fracture that results in material removal. This fact also explains why the substrate, with hardness Hv 240, has higher abrasion resistance than several coatings with hardness up to Hv 800 (Fig. 2).

Figure 5(e) and (f) compare the abrasive wear behavior of two samples with low hardness. SN2 (Fig. 5e) is a bimodal coating deposited with low-temperature HVOF. It contains 98% retained WC and has relatively high abrasion resistance (Fig. 2). Sample R6 (Fig. 5f) is a Nanocarb powder deposited by HVOF. It has 91.5% retained WC, quite low decarburization, and low abrasion resistance. The difference in the abrasion behavior of these two samples (Fig. 5e and f) is that SN2 experiences fracture on a small scale and R6 shows a mixture of plastic deformation of large “particles,” fracture on a scale of about 30 μm , and loose, small wear debris, visible in the center of Fig. 5(f). Examination of the microstructures of these coatings, in Fig. 3(a) and (b), reveals that SN2 is composed of a mixture of micro-

scopic and submicron grains and that the binder phase (Co) is missing between many of the grains, forming a nanoscale porosity. This feature is responsible for the low hardness of the sample and explains the “crumbling” that characterizes the scratch in Figure 6(d) and the shape of the abraded surface. Sample R6 in Figure 3(b) is likewise composed of many rounded particles with missing binder phase between them. Each one of these particles is a small agglomerate of nanoscale WC grains. The larger particle, on the upper left, is a well-bonded agglomerate of nanoscale particles (from high-resolution SEM, not shown). In the abraded surface R6, the plastically deformed particles are the well-bonded agglomerates that are easily broken away from the material. The samples R6 and R24 are the only ones in which we have observed small, loose wear debris in abrasion.

It is worth noting that, in all our measurements, the coatings adhered well to the substrate. No case of debonding of the coating was observed in sliding, abrasion, and scratching.



4. Conclusions

Reviewing the information obtained from microstructure, composition, scratching, sliding, and abrasive wear, we obtain the following picture.

The properties and performance of the coatings studied here depend more on the deposition technique than on the starting powder used. Table 1 shows no correlation between the cobalt content or the WC grain size of the powders with the hardness, sliding, or abrasion resistance of the coatings. Low-temperature deposition produces porous coatings with poor adhesion between the particles. Decarburization of the coating produces brittle phases 20 to 100 μm in extension, which increase the hardness of the coating but cause sliding and abrasive wear by removal of large plates.

Nanostructured powders used for the coatings in the present study had the shape of hollow spheres. They rapidly reached high temperatures in the various deposition processes and were subject to extensive decarburization. If it is possible to produce nanostructured powders in solid agglomerates, similar to the commercial powders, it may be possible to deposit these materials under conditions that avoid decarburization. This may, however, present a challenge because of the large surface-to-volume ratio of WC crystal.

The data show that multimodal coatings, produced from mixed powders, present an exciting opportunity, especially in abrasive wear, which is more sensitive to microstructure than sliding wear.^[4]

Acknowledgments

The authors thank the Office of Naval Research for providing funding under Grant No. N00014-98-3-0005. They also express their gratitude to Professor Bernard Kear for many stimulating discussions and the many colleagues who provided the coatings. They are not named here because of the large differences in the performance of these experimental coatings.

References

1. L.E. McCandlish, B.H. Kear, and B.K. Kim: *Mater. Sci. Technol.*, 1990, vol. 6, pp. 953-60.
2. K. Jia, T.E. Fischer, and G. Gallois: *NanoStruct. Mater.*, 1998, vol. 10, pp. 875-91.
3. K. Jia and T.E. Fischer: *Wear*, 1994, vol. 203-204, pp. 310-18.
4. K. Jia and T.E. Fischer: *Wear*, 1996, vol. 200, pp. 206-14.
5. V. Ramnath and N. Jayaraman: *Mater. Sci. Technol.*, 1989, vol. 15, pp. 382-88.
6. Saifi Usmani and Sanjay Sampath: *Tribol. Trans.*, 1997, vol. 40 (3), pp. 470-78.
7. H.L. de Villiers Lovelock: *J. Thermal Spray Technol.*, 1998, vol. 7 (3), pp. 357-373.
8. C.J. Li, A. Ohmori, and Y. Harada: *J. Mater. Sci.*, 1996, vol. 31, pp. 785-94.
9. C.J. Li, A. Ohmori, and Y. Harada: *J. Thermal Spray Technol.*, 1996, vol. 5 (1), pp. 69-73.
10. S. Wantanabe, T. Tajiri, N. Sakoda, and J. Amano: *J. Thermal Spray Technol.*, 1998, vol. 7 (1), pp. 93-96.
11. J. Voyer and B.R. Marple: *Wear*, 1990, vol. 225-229, pp. 135-45.
12. I. Grimberg, K. Soifer, B. Bouaifi, U. Draugelates, and B. Z. Weiss: *Surface Coatings Technol.*, 1997, vol. 90, pp. 82-90.
13. J.M. Guilemany, L. Delaey, F.J. Sanchez, and L. Jacobs: *La Metallurgia Italiana*, 1996, vol. 88 (2), pp. 133-36.
14. H. Kreye, R. Schwetzke, and S. Zimmermann: in *Thermal Spray: Practical Solutions for Engineering Problems*, C. C. Berndt, ed., ASM International, Materials Park, OH, 1996, pp. 451-56.
15. R.J. Thorpe and M.L. Thorpe: in *Thermal Spray: Research, Design and Applications*, C. C. Berndt and T. F. Bernecki, eds., ASM International, Materials Park, OH, 1993, pp. 69-78.
16. J. Nerz, B. Kushner, and A. Rotolico: in *Protective Coatings: Processing and Characterization*, R. M. Yazici, ed., TMS, Warrendale, PA, 1990, pp. 135-43.
17. T.A. Mantyla, K.J. Niemi, P.M. J. Vuoristo, G. Barbezat, and A.R. Nicoll: *2nd Plasma-Technik Symp.*, S. B. Sandmeier, P. Huber, H. Eschnauer, and A. Nicoll, eds., Lucerne, Switzerland, Plasmatechnik, Wohlen, Switzerland, 1991, vol. 1, pp. 287-97.
18. M.R. Dorfman, B.A. Kushner, J. Nerz, and A.J. Rotolico: *Proc. 12th Int. Thermal Spray Conf.*, I. A. Buclow, ed., The Welding Institute, London, 1989, p. 108.
19. K.V. Rao, D.A. Somerville, and D.A. Lee: *Advances in Thermal Spraying*, Pergamon Press, Elmsford, NY, 1986, pp. 873-82.
20. H.M. Hawthorne, B. Arsenault, J.P. Immrigeon, J.G. Legoux, and V.R. Parameswaran: *Wear*, 1999, vol. 225-229, pp. 825-34.
21. S.F. Wayne and S. Sampath: *J. Thermal Spray*, 1992, vol. 1 (4), pp. 307-15.
22. D.A. Stewart, P.H. Shipway, and D.G. McCartney: *Wear*, 1999, vol. 225-229, pp. 789-98.
23. J. Subrahmanyam, M.P. Srivastava, and R. Sivakumar: *Mater. Sci. Eng.*, 1986, vol. 84, pp. 209-14.
24. J. Nerz, B. Kushner, and A. Rotolico: *J. Thermal Spray Technol.*, 1992, vol. 1 (2), pp. 147-52.
25. R.J.K. Wood, B.G. Mellor, and M.L. Binfield: *Wear*, 1997, vol. 211, pp. 70-83.
26. A. Karimi, C. Verdon, and G. Barbezat: *Surface Coating Technol.*, 1993, vol. 57, pp. 81-89.
27. H. Nakahira, K. Tani, K. Miyakima, and Y. Harada: in *Thermal Spray: International Advances in Coatings Technology*, C. C. Berndt, ed., ASM International, Materials Park, OH, 1992, pp. 1011-17.
28. Herbert Herman: *Scientific Am.*, 1988, Sept., pp. 112-17.
29. H. Taikawa, H. Hirata, M. Koga, M. Itoh, and K. Takeda: *Surface Coating Technol.*, 1989, vol. 39-40, pp. 127-34.
30. J.M. Guilemany, J. Mutting, and J.M. de Paco: *Proc. 4th Eur. Conf. Adv. Mater. Processing*, 1995, pp. 25-28.
31. G. Skandan, R. Yao, R. Sadangi, B.H. Kear, Y. Qiao, L. Liu, and T.E. Fischer: *J. Thermal Spray Technol.*, 2000, vol. 9, pp. 329-31.
32. M.M. Krushov: *Proc. Conf. on Lubrication and Wear*, IMME, London, 1957, p. 199.
33. M.M. Krushov: *Wear*, 1974, vol. 28, p. 69.